

Reservoir Rock Characterization Using Wavelet Transform and Fractal Dimension

*Partovi, Seyyed Mohammad Amin; Sadeghnejad, Saeid***

*Department of Petroleum Engineering, Faculty of Chemical Engineering, Tarbiat Modares University,
Tehran, I.R. IRAN*

ABSTRACT: *The aim of this study is to characterize and find the location of geological boundaries in different wells across a reservoir. Automatic detection of the geological boundaries can facilitate the matching of the stratigraphic layers in a reservoir and finally can lead to a correct reservoir rock characterization. Nowadays, the well-to-well correlation with the aim of finding the geological layers in different wells is usually done manually. For a rather moderate-size field with a large number of wells (e.g., 150 wells), the construction of such a correlation by hand is a quite complex, labor-intensive, and time-consuming. In this research, the wavelet transform as well as the fractal analysis, with the aid of the pattern recognition techniques, are used to find the geological boundaries automatically. In this study, we manage to use the wavelet transforms approach to calculate the fractal dimension of different geological layers. In this process, two main features, the statistical characteristics as well as the fractal dimensions of a moving window, are calculated to find a specific geological boundary from a witness well through different observation wells. To validate the proposed technique, it is implemented in seven wells of one of the Iranian onshore fields in the south-west of Iran. The results show the capability of the introduced automatic method in detection of the geological boundaries in well-to-well correlations.*

KEYWORDS: *Wavelet transform; Fractal; Geological boundary; Pattern recognition; Well-log.*

INTRODUCTION

The main purpose of reservoir characterization is constructing a three-dimensional model of a reservoir (i.e., geological model) that can be representative of rock and fluid properties of the porous media under study. Such a reservoir model is required to optimize well placement [1] and to design an optimal plan for oil and gas reservoir development in its early stages [2,3]. In this regard, a variety of input data should be used including well-log, core analysis, two and three-dimensional seismic, reservoir fluid properties, pressure testing,

production, etc. [4]. Among these data, core analysis, petrophysical data, and geophysical data play the most important role in reservoir characterization and especially in well-to-well correlation. Coring operation is not usually implemented in all wells and seismic acquisition is done just on a section of a field in most cases. However, logging results are available in most of the wells. Therefore, in well-to-well correlation, a method that can stratigraphically characterize a reservoir by implementing the well-log data is quite valuable [5].

* To whom correspondence should be addressed.

+ E-mail: sadeghnejad@modares.ac.ir

1021-9986/2018/3/223-233

11/\$/6.01

In well-to-well correlation, finding the depth of a specific geological layer among different wells is usually done manually by implementing some visual and qualitative analyses. The accuracy of boundary detection depends on the amount of experience of the analyzer; therefore multi-interpretation by several interpreters is not unexpected. Analyzing hundreds of wells in a field requires a lot of time and in geologically complicated fields, the process sometimes becomes even impracticable. The existence of discontinuities e.g., faults, pinch-outs, make this process more difficult. Furthermore, this process becomes a slow procedure. While automated method provides total well-to-well correlation just in several minutes. Implementing a computer-based program, which is able to automatically afford the well-to-well correlation can facilitate the reservoir characterization process. High speed, low cost, and preventing from multi interpretations are the benefits of our automated method compared to the manual ones.

In the past three decades, the methods of automatic geological boundary detection have had remarkable progress. The use of dynamic programming, pattern recognition, and wavelet transform approaches are some efforts to achieve the desired well-to-well correlation. Rivera Vega used wavelet transform to interpret the phenomenon of depositional cycles in logs and core data from a well in a fluvioeolian sequence in Ormskirk Sandstone, Irish Sea. The boundary detection technique was tested using log data from 10 wells in the Apiay field, Colombia [6]. Zoraster *et al.* implemented the dynamic programming approach in well-to-well correlation to determine geological boundaries with regard to the changes that may be present in the thickness of the layers [7]. Yuan in 2013 processed the data of the late Permian coal-bearing strata in western Guizhou. The study mainly focused on the controlling effects, which Milankovitch had on the high-frequency sequence. The Milankovitch cycle can be used as a ruler of sequence stratigraphy division and correlation to ensure the scientificity and the unity of sequence stratigraphy division [8]. Perez-Muñoz implemented a wavelet transform of gamma ray, resistivity, and sonic logs to recognize geological layers of Chicontepec formation, Mexico. They calculated wavelet transform coefficients along the well and considered points that contain higher wavelet energy as the shale layers, while the low energy

indicated the presence of sandstones and medium energy indicated the sandstone-shale intercalation [9]. Lapkovsky in 2015 considered a variant of automatic correlation between good sections based on the construction of multidimensional functions of differences between fragments of logs. A multidimensional-difference function was constructed which is used to compare each well simultaneously with the totality of its surrounding wells and optimize the correlation solution by minimizing this difference. The well-log correlation model is obtained by constructing the optimal trajectory in the field of the distance function [10]. The optimal line was constructed using an ant colony algorithm [11] and a wave algorithm [12]. The points of this line were the values of pairs of depths of the wells being compared that are minimally different from each other according to the set of log curves used. In 2016, Subhakar and Chandrasekhar carried out fractal and multi-fractal analysis of neutron and gamma logs using Detrended Fluctuation Analysis (DFA) to find out geological boundaries [13]. Ye *et al.* provided a semi-automated method based on well-log pattern recognition. The CWT phase image exhibits oval-shaped after mirroring. A Significance-of-Cone (SOC) method has been developed to extract the boundary information [14]. In 2017, Kadkhodaie and Rezaee used Continuous Wavelet Transform (CWT) to decompose gamma ray and porosity log into a set of wavelet coefficient. A Discrete Wavelet Transform (DWT) is utilized to decompose well-logs into smaller frequency bandwidths called approximation and details. Sequence boundary recognized through hybridizing bot CWT and DWT coefficient [15].

The aim of this study is to implement an automated method for well-to-well correlation. The statistical features, as well as the Fractal dimension of the log signals through a sliding-window approach, are used to encounter the associated geological boundaries among multiple wells. This approach is tested on well-log data of one of the Iranian onshore fields. The geological features of the witness well are searched through the next six observation wells. For computing the Fractal dimension of each well-log window, the Wavelet transform analysis is used.

To present this study, this manuscript has been organized as follows. First, the wavelet transform is introduced and then the idea of using self-similar shapes

and fractal dimension is presented. Following the primary definition of the mathematical tools in this study, the calculating method of the fractal dimension by wavelet transform is described in detail. It is followed by testing the applicability of the introduced automated approach in one of the Iranian fields.

WAVELET TRANSFORM

What is called the wavelet analysis is a tool for transformation that has the capability to decompose a time-domain signal into a set of basic functions called wavelet basis. The wavelet basis functions are obtained by dilating and translating of a mother wavelet function. The result of the wavelet transform is some wavelet coefficients, which is the function of position and scale. By multiplying each of these coefficients by the child wavelet, the input signal can be restored. The wavelet transform, $WT(f(t))$, of a signal like $f(t)$ in time dimension is as follows:

$$WT(f(t)) = \int_{-\infty}^{+\infty} f(t) \psi_{a,b}^*(t) dt \quad (1)$$

Where, sign “*” denotes the complex conjugate of function. In the above equation, $f(t)$ is the signal of interest, $\psi_{a,b}(t)$ is the analyzer wavelet function. The wavelet functions known as child functions are obtained by dilating, a , and translating, b , of a mother wavelet, ψ , [16, 17].

$$\psi_{a,b}(t) = \frac{1}{\sqrt{a}} \psi\left(\frac{t-b}{a}\right) \quad (2)$$

In order that a function is selected as a wavelet basic function, it must have some specific conditions. The first condition is known as admissibility condition [16].

$$\int_0^{+\infty} \frac{|\hat{\psi}(\omega)|^2}{|\omega|} d\omega = \int_{-\infty}^0 \frac{|\hat{\psi}(\omega)|^2}{|\omega|} d\omega = C_{\hat{\psi}} < \infty \quad (3)$$

Where ω is the frequency of mother wavelet in the Fourier domain. It can be proved that such a function, ψ , that has the admissibility condition can be used for wavelet transform without losing any information during the transformations [16]. This condition indicates that the Fourier transform of mother wavelets in frequencies close to zero disappear. In other words:

$$\lim_{\omega \rightarrow 0} |\hat{\psi}(\omega)|^2 = 0 \quad (4)$$

Which shows that the frequency component of the function is not zero. Zero at frequencies close to zero means that in time dimension the average of mother wavelet function must be zero:

$$\int_{-\infty}^{+\infty} \psi(t) dt = 0 \quad (5)$$

In other words, the mother wavelet function must be fluctuating to satisfy the above condition.

The mother wavelet function must have limited energy in the time dimension [17].

$$E = \int_{-\infty}^{+\infty} |\psi(t)|^2 dt < \infty \quad (6)$$

The wavelet transform function has at least one vanishing moment [17]. Mother wavelet function has d vanishing moments if and only if for all non-negative integer number, q , that $q < d$ we have:

$$\int_{-\infty}^{+\infty} t^q \psi(t) dt = 0 \quad (7)$$

The wavelet transforms analysis is a new mathematical method instead of the conventional Fourier analysis [16, 17]. Today, two kinds of the wavelet transform, Continuous Wavelet Transform (CWT) and Discrete Wavelet Transform (DWT) have been developed. Sometimes Discrete Wavelet Transform called orthogonal wavelet transform. The reason is the use of orthogonal functions in discrete wavelet transform.

FRACTALS AND SELF-SIMILAR SHAPES

The vast amount of the literature in the past decade was dedicated to analyzing dynamic systems and their physical governing relations. The success in this area depends on the predictability of the system behavior. The Euclidean geometry, which based on lines and regular geometric shapes, is a powerful tool to analyze the governing relation of these systems. In addition, differential equations play an important role in studying the growth of such systems. However, the natural phenomena such as mountains, clouds, and trees cannot be expressed exactly by this regular geometrics in the Euclidean geometry. In the past decades, understanding

the behavior of such systems has had great development. The Fractal geometry is indicative of the behavior of complex shapes that are scattered throughout the universe. Until now, there is not any common definition of what is called fractal, but it is clear that fractal shapes are very different from Euclidean shapes [18]. Fractals are natural phenomena that have a self-similar property in different size scale, which is hidden behind a quite irregular shape.

The Fractal dimension is the most important key factor of any type of fractal phenomena since it contains information about the geometry of self-similar shapes. There are several definitions available for fractal dimension, but these dimensions are not easy to calculate. A number of different parameters to describe the properties of fractals have been introduced (e.g. fixed Hurst parameter Hausdorff etc.).

If a self-similar shape was formed by N copies of itself, which each one has a magnification factor of r , then the parameter of self-similarity or the fractal dimension is obtained from the following definition:

$$D = \frac{\text{Log}(N)}{\text{Log}(r)} \quad (8)$$

Using the box-counting method [19] fractal dimension is the slope of the line when we plot the value of $\text{Log}(N)$ on the Y-axis against the value of $\text{Log}(r)$ on the X-axis. This definition for a straight line results one and for a square results two.

The self-similarity characteristic can be divided into two categories, deterministic fractals, and random fractals. In the first group, there are two major categories: the exactly self-similar fractals and the statistical fractals. The random fractals are shapes that generated randomly or by chance but the exactly self-similar fractals can be expressed by a precise formula. The exactly self-similar shapes can be divided into finer pieces as each of these pieces are exactly the same as the main shape [20]. In Fig. 1 a Mandelbrot set with a continuously colored environment is presented as a fractal shape.

The mathematical model that can express the characteristics of the statistical fractals is expressed by the fractional Brownian motion (fBm), which is widely used to model the random fractals [21]. For the first time, fBm was introduced by *Mandelbrot* and *Van Ness* in 1968 [22] and until now it has been used to model many

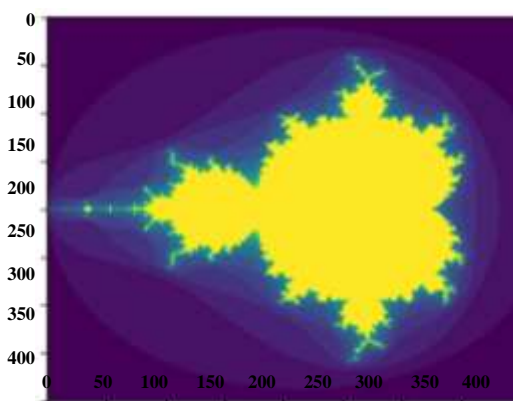


Fig. 1: Mandelbrot set as a complex fractal shape.

scientific phenomena. The fractal Brownian motion is a generalization of the Brownian motion, just as the Brownian motion has its own specific characteristics. If fBm is specified by B_H function then this function shows a unique process which has the following general characteristics [23, 24]:

- 1- Is a Gaussian process with zero mean in which $B_H(0) = 0$
- 2- Is a statistical self-similarity process with Hurst parameter (a kind of fractal dimension), $0 < H < 1$. (λ is a constant number)

$$B_H(\lambda t) = \lambda^H B_H(t) \quad (9)$$

- 3- It has stationary increment characteristic.

According to the conditions, (2) and (3), fBm is a self-similar process with stationary increments. The second condition dictates that the above process is not static. As mentioned, fBm is a generalization of the Brownian motion model or Gaussian noise [25].

$$B_H(t) = \frac{1}{2\pi} \int_{-\infty}^{+\infty} \frac{1}{(i\omega)^{H+0.5}} (e^{i\omega t} - 1) dB(\omega) \quad (10)$$

Where $B(\omega)$ in the above equation is the usual Brownian motion.

FRactal ANALYSIS BY WAVELET TRANSFORM

There are several methods for computing of the fractal dimension: Power spectrum method [19], Variance method [19], Wigner-Ville description method [19, 22], Differencing variance method, Aggregated variance

method [26], Welch periodogram [22], Higuchi method [27], Whittle method are such examples [26, 28]. The typical method of calculating fractal dimension is implementing the wavelet transform. The wavelet transform has this capability to zoom in and out on a signal in different scales with the help of its mathematical methodology. In other words, when a signal shows a self-similar behavior in different size scales, it is possible to detect this behavior by using wavelet transform [24, 25].

In this study, the Hausdorff dimension (i.e., a fractal dimension) is used to determine the self-similar characteristic of the well-log. To calculate the Hausdorff parameter, the following process can be implemented [29]:

- 1- Select a sequence of scales, $a_1 > a_2 > \dots > a_k$, say $a_j = 2^{-j}$, where $j = 1, \dots, k$.
- 2- Define a set of bi-variant data $(x_j; y_j)$, $j = 1, \dots, k$, by setting.

$$x_j = \text{Log}(a_j) \quad \& \quad y_j = y_t(a_j) \quad (11)$$

- 3- Estimate of the H_a parameter by regression.

$$H_a(t) = \frac{\left(\frac{\sum (x_j - \bar{x})(y_j - \bar{y})}{\sum (x_j - \bar{x})} - 1 \right)}{2} \quad (12)$$

Where \bar{x} and \bar{y} are the averages of x_j and y_j . H_a in the above equation is the Hausdorff dimension.

Since each geological layer has a specific behavior in terms of the rock properties; therefore, the fractal dimension of well-log obtained for that layer expected to be almost identical. In a better word, the different layers of a reservoir act as a series of several fractal signals. In fact, well-logs of different layers act as a multi-fractal behavior [30,31]. Therefore, the fractal dimension of each geological layer has its own value, which is different from other adjacent layers. Calculating the fractal dimension of two different layers, they can be easily recognized.

AUTOMATED PROCEDURE FOR GEOLOGICAL BOUNDARY DETECTION

The purpose of this study is to evaluate the performance of a novel method in well-to-well correlation. To detect geological boundaries, a sliding window approach is adapted from a study by *Rivera Vega* [6].

A window is placed on the well-log of the witness well as its center coincides with the selected boundary. Two signals, one in the top and one at the bottom of the window are available. As the geological layers have different signal features, the idea is finding both the statistical characteristics as well as the fractal behavior of these features in witness well and searching for the same behavior in the observation wells (Fig 2).

The statistical features for analyzing the upper and lower windows were selected from *Rivera Vega* [6]. The first feature is the signal average that calculated for the upper and lower windows,

$$\bar{f}^{\text{Upper or Lower}} = \frac{\sum_{i=1}^b f_i}{b} \quad (13)$$

Where b is the number of well-log data in the upper or lower window. The next feature is the coefficient of variation, which is calculated as follows:

$$Cv^{\text{Upper or Lower}} = \frac{\sqrt{\text{var}(f^{\text{Upper or Lower}})}}{\bar{f}^{\text{Upper or Lower}}} \quad (14)$$

in which, var is the variance of the signal. As the coefficient of variation is a dimensionless number, it is preferred to the variance and standard deviation.

The maximum to minimum ratio is the next feature, which can be an indicator of the intense changes in the signal. This parameter may contain information of shale-to-sand ratio.

$$f_{\text{max/min}}^{\text{Upper or Lower}} = \frac{\max(f_i^{\text{Upper or Lower}})}{\min(f_i^{\text{Upper or Lower}})} \quad (15)$$

In addition to the introduced statistical parameters, the most important key parameter, which is considered for both parts of the upper and lower window is the Hausdorff parameter. As aforementioned, this fractal dimension is calculated using the methodology described in the last section based on the wavelet transform. Computation of this parameter in conjunction with the statistical coefficients is the main idea of this study. To achieve this, the upper and lower parts of the sliding window are decomposed in the wavelet domain to different size scales and consequently, the fractal dimension (i.e., Hausdorff parameter) of each sub-window will be calculated.

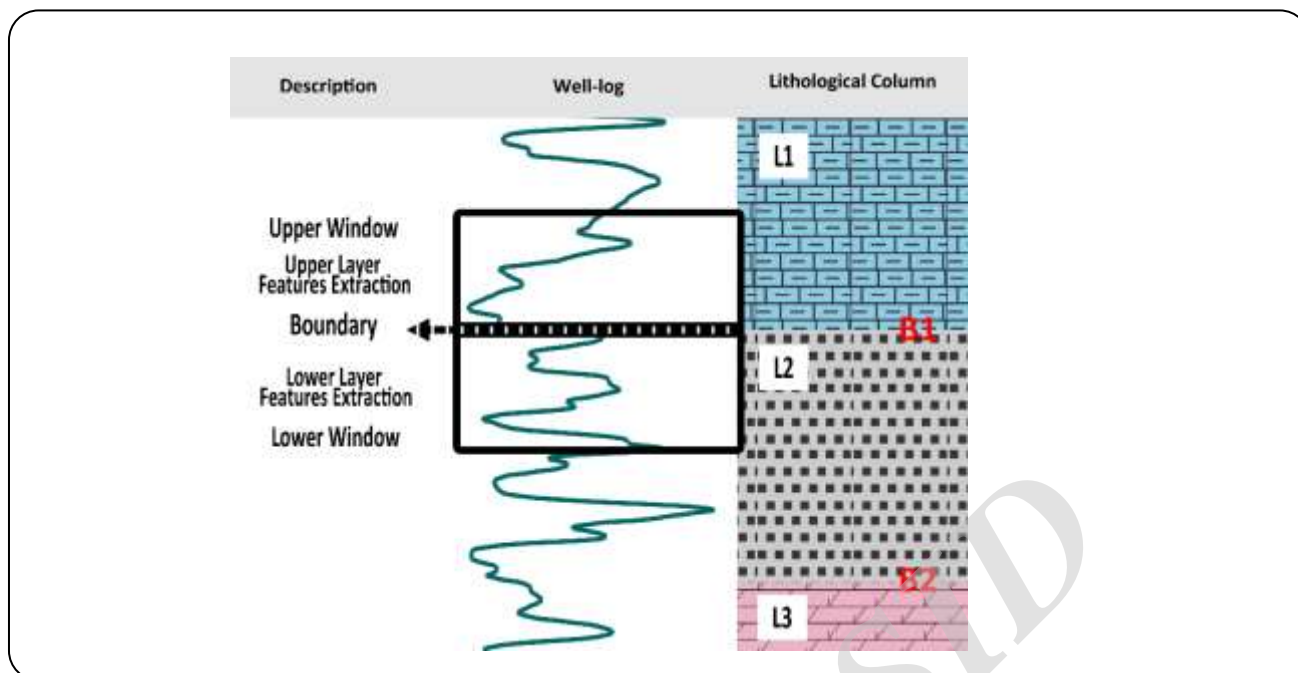


Fig. 2: Schematic of a window around the selected geological boundary (B1 boundary between stratigraphic layers of L1 and L2) in witness well. The features of the well-log signal are calculated at both sides of the boundary (i.e., lower and upper windows).

The principal assumption is the multi-fractal behavior of each layer in the sub-windows.

Subsequent to the calculation of the statistical parameters as well as the fractal dimension of the upper and lower sub-window for a specific geological layer in the witness well, the algorithm searches for the same layer in the other wells (observation wells) of the field. The search process is based on the moving of a window with the same size in the witness well along the entire length (depth) of the observation wells. The schematic of searching in the observational wells is depicted in Fig. 3.

Our algorithm automatically searches for a specific depth in the observation wells that has the same statistical parameters as well as the fractal dimension as was previously observed in the witness well for the selected boundary (i.e., geological boundary). The depth in the observation wells that has identical properties as the boundary in the witness well is considered as the same geological boundary. The algorithm continues to detect the other boundaries of the formations in the witness well among the observations wells. In order to calculate the similarity probability of the features of the selected geological layer in the witness well with different locations of the observation wells (i.e., the positions of the moving window along the observation well depth),

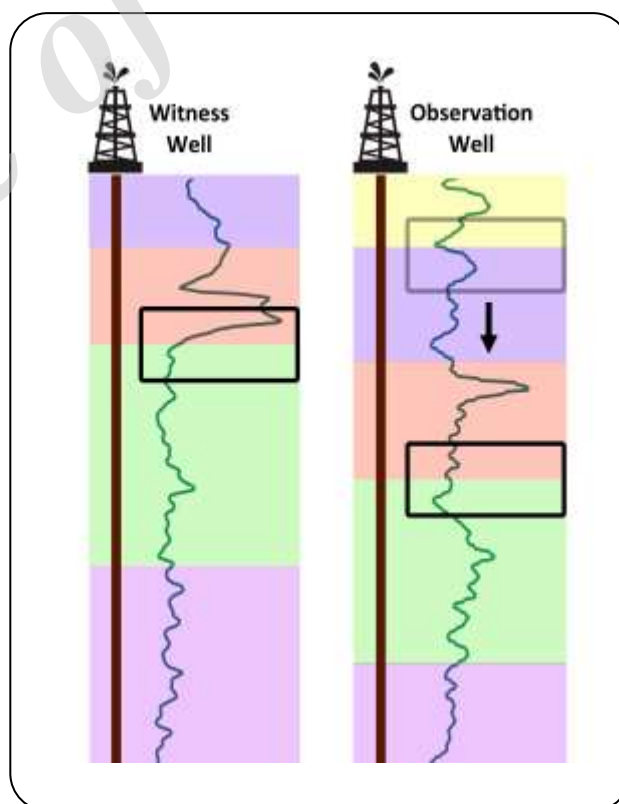


Fig. 3: The features calculated along the entire length (depth) of the observation wells in a sliding window with the same size of the window used in the witness well.

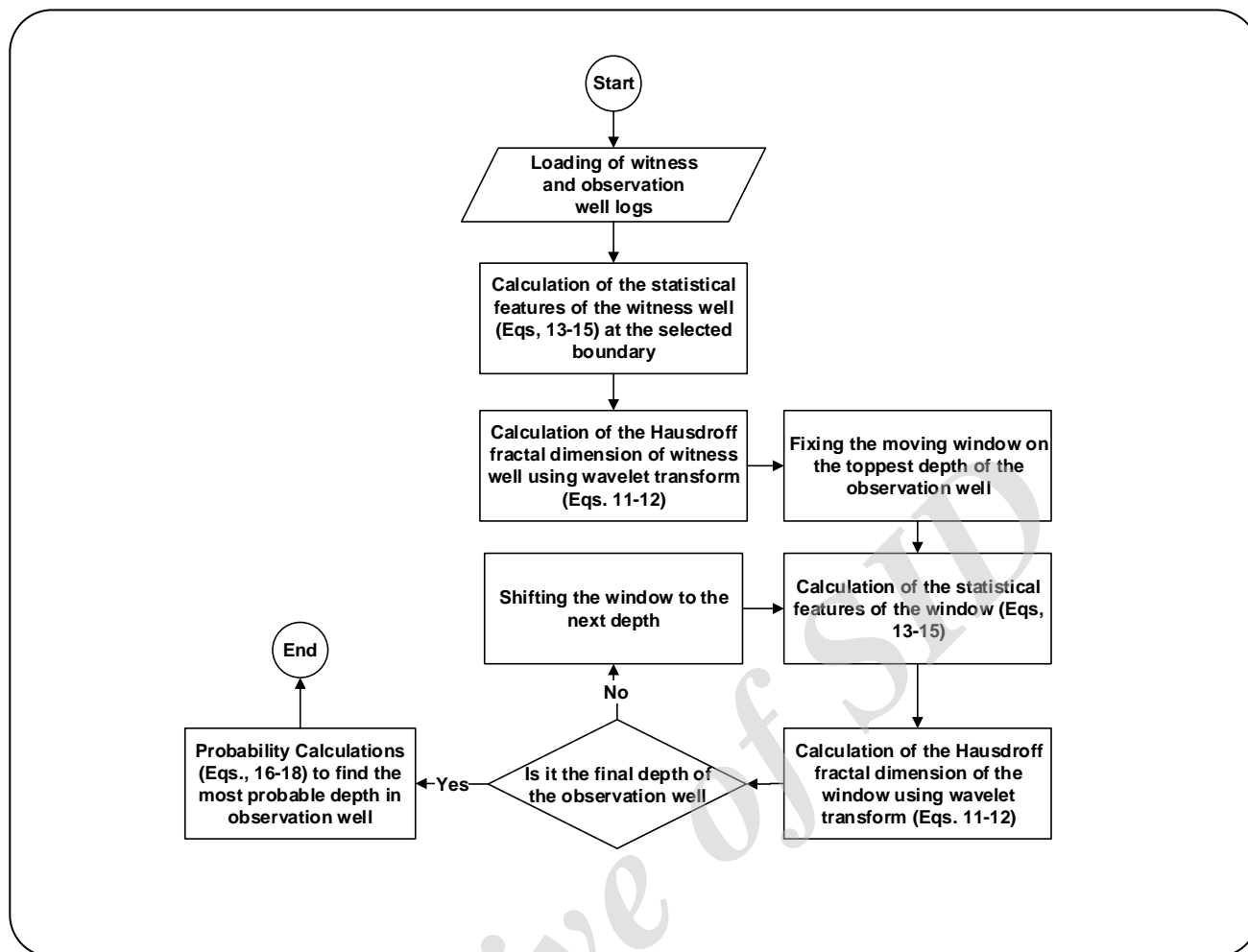


Fig. 4: The flowchart of the implemented algorithm.

an error matrix was defined. This matrix is formed by subtracting the value of the feature calculated in the witness well, WF , from the observation wells one, OF_i .

$$E_{i,k} = WF - OF_i \quad i = 1, 2, \dots, NDP \quad (16)$$

Where NDP is the number of windows along the observation well. If the calculated features, $k = 1, 2, \dots, f$ (which f is the number of features: equations 12 to 15), are independent of each other, then the conditional probability that each depth of the observation well be identical to the selected boundary in the witness well can be computed as,

$$P(O|W_i) = \prod_{k=1}^f P(O_k|W_{i,k}) \quad (17)$$

Assuming the Gaussian distribution for the error with the average of zero and standard deviation of σ ,

the conditional probability for each depth of the witness well that is similar to the selected boundary in the witness well for a specific feature, k , can be calculated as,

$$P(O_k|W_{i,k}) = \frac{1}{\sqrt{2\pi\sigma_k^2}} \exp\left(\frac{-E_{i,k}}{2\sigma_k^2}\right) \quad (18)$$

Fig. 4 shows the flowchart of the analysis. It is worth mentioning that all the analyses were implemented in MATLAB software package.

CASE STUDY

To validate the introduced methodology, data of one of the Iranian onshore fields were used as a case study (Fig. 5). This field is a rather long and asymmetric anticline with a length of about 22.5 km and width of 4.5 km, which is located at 7km of northeast of Ahwaz. In 1970, the existence of oil in this field has been proved

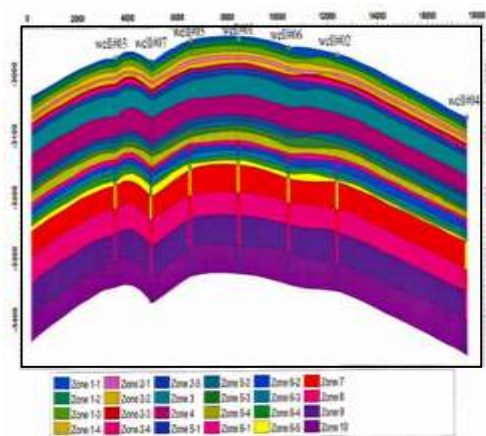


Fig. 5: The structural cross-section map of the field under study.

by drilling the first well. The total volume of oil in place and recoverable oil are 2308 and 542 million barrels, respectively. The estimated API of the field is between 28 and 36. The oil is produced from the Asmari formation, which is between 370 to 400 meters thick. The formation rock is composed of limestone, dolomite, sandstone and shale stone. About 70% of the total amount of hydrocarbon is stored in sandstone. The average value of the porosity and water saturation in this field is about 23.7% and 27.7%, respectively. Because of the low dip of the anticline limbs, the existence of the fractures is less probable. The field is divided into 4 layers. The first and third layers contain oil and the second and fourth layers contain water. As shown in Fig. 5, each layer composed of several main zones and sub-zones. As an example, the introduced well-to-well correlation algorithm was implemented to find the boundary that separates the two sub-zones of Z6-1 and Z6-2. This boundary is located in the third layer, Asmari, and is at the interface of water-oil-contact. This 80 meters thick layer composed of 34 meters sandstone and 11 meters shale stone and the rest is dolomite and limestone.

Among the available well-log, the Gamma-ray log, which is available in all wells of the field, was used as the input signal in this study (Fig. 6). "Heterogeneity" as the variability of an individual or combination of properties including sedimentological characteristics and fractures [32] can affect well-to-well correlation results either in manual or automated methods. However, using another

source of data, such as other well-logs and core analysis can amplify automated well-to-well correlation especially in the heterogeneous fields.

RESULTS AND DISCUSSION

To validate the introduced algorithm on real data the well #01 is considered as the witness well and the boundary at the depth of 3131.9 meters which separates Z6-1 from Z6-2, was considered. The aim of this case study is to detect this boundary in the rest of the observation wells.

Fig. 7 is an example of our program output in Matlab. From left to right the figure depicts the witness well-log, that the selected boundary is indicated by the horizontal line across it; the middle graph shows the observation well logs, and the right figure is the normalized probability along the depth of the observation well. The higher probability value in the third figure indicates that its corresponding depth has a greater chance to be identical with the selected geological layer of the witness well. Size of the moving window has great importance, in order to detect the exact depth of the boundaries and to avoid the influence of the adjacent layer in the estimation of the parameters in the thin layers; calculation must be done within a window, which its size is not larger than the thickness of the geological layers. In this analysis, by checking the thickness of the layers in the witness well, the appropriate length of the moving window was considered fixed as 10 meters.

According to the normalized probability graph, the depth of 3053.5 meters in the observation well has the greatest probability i.e. it has the closest match to the selected depth (geological boundary) in the witness well. Comparing the results obtained from the new automatic algorithm in Well #02 with the manual well-to-well correlation reports available from the field data shows that there is only a 0.5 meters deviation between these two results. Table 1 summarizes the results of our implemented algorithm in comparison with the manual Results of the well-to-well correlation in the field under study.

It can be seen that the results of the developed algorithm used in this study are in complete agreement with the conventional manual well-to-well correlation techniques. The average deviation of results is about 1.06 m, which is quite acceptable. Considering the aforementioned benefits of the developed automatic pattern recognition

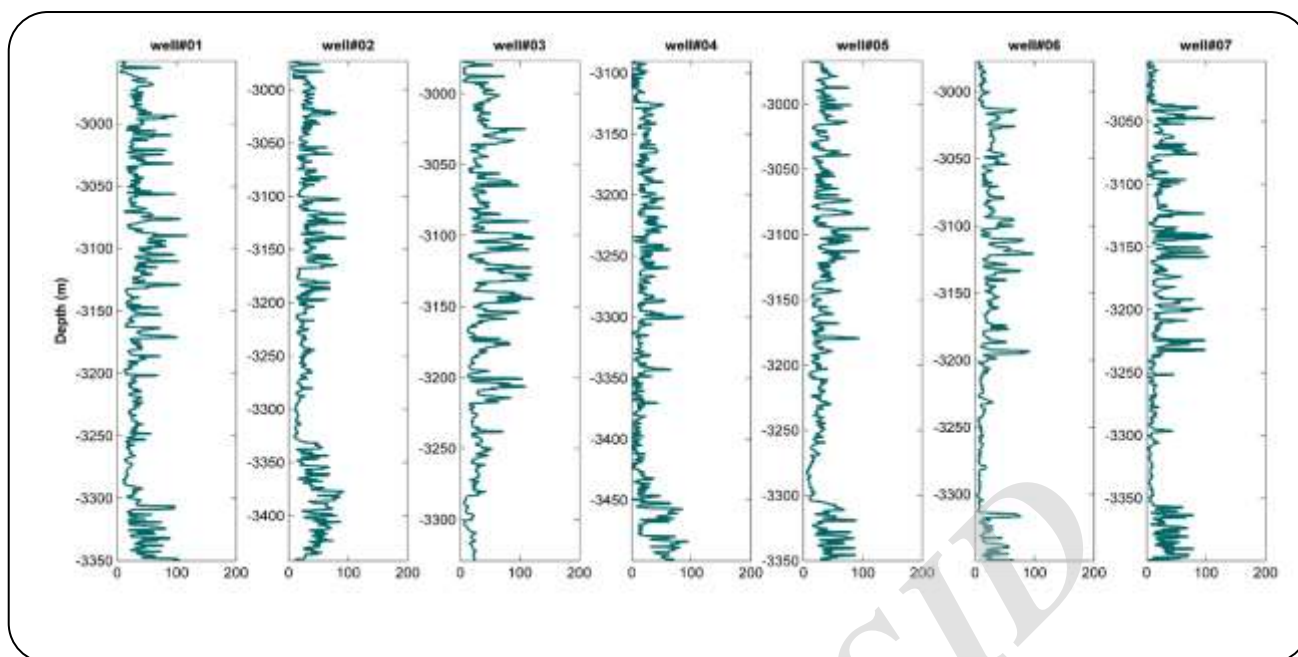


Fig. 6: Gamma-ray log of all wells in the field under study, X-axis unit is GAPI.

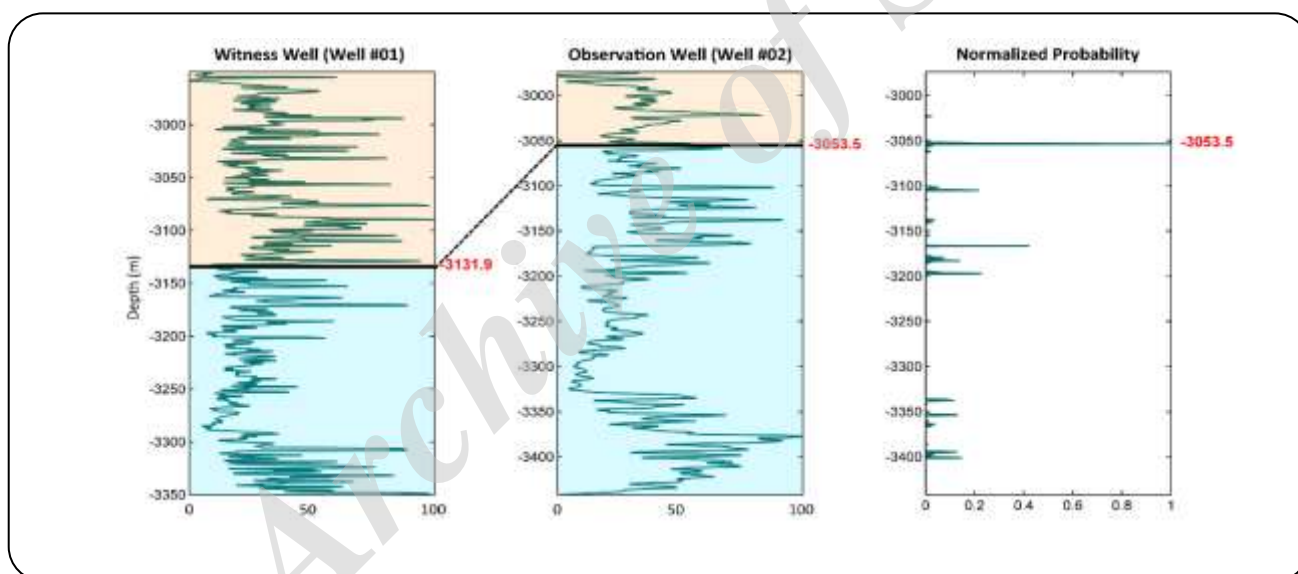


Fig. 7: Output of the introduced program, left: Gamma-ray data of the Well#01 (witness well), middle: Gamma-ray of Well#02 (observation well) right: normalized probability along the observation well

a technique to decrease the time of the analysis proves the capability and applicability of this method in the automatic analyses of the well-to-well correlations.

CONCLUSIONS

This study was focused to implement an automated algorithm to find geological boundaries during well-to-well correlation with the help of the pattern recognition

method. Computing some key characteristics of a window around the selected boundary in the witness well and searching for the same window in the observation wells is the main algorithm of this methodology. In addition to some statistical features, the fractal dimension was used as the characteristic properties of the well-log signals. In addition, the discrete wavelet transform method was used to calculate the Hausdorff fractal dimension.

Table 1: Summary of the result for finding the selected boundary with the automatic pattern recognition-based method in comparison with the conventional manual well-to-well correlation method

Well Name	Well Type	Depth of the boundary from the manual approach (m)	Calculated depth of the boundary by the automatic method (m)	Deviation (m)
Well # 01	Witness	3131.9	-	-
Well # 02	Observation	3035.0	3035.5	+0.5
Well # 03	Observation	3160.0	3162.9	+2.9
Well # 04	Observation	3260.8	3261.1	+0.3
Well # 05	Observation	3134.0	3133.0	-1.0
Well # 06	Observation	3140.0	3137.5	-2.5
Well # 07	Observation	3176.0	3177.2	+1.2

The presented algorithm is able to detect automatically the geological boundaries of the witness well in the other observation wells. One of the advantages of this method is the lack of influence of the real changes in the thickness of layers or the discontinuities across the formation. Furthermore, the automatic feature of this method can eliminate inconsistencies in the manual methods and can facilitate the well-to-well correlation process. The results obtained from the use of this algorithm on a real case study on one of the Iranian fields were confirmed the less computing time and the overall effectiveness of this method.

Received : Feb. 12, 2016 ; Accepted : Aug. 20, 2017

REFERENCES

- [1] Afshari S., Aminshahidy B., Pishvaie M.R., [Well Placement Optimization Using Differential Evolution Algorithm](#), *Iranian Journal of Chemistry and Chemical Engineering (IJCCE)*, **34**(2): 109-116 (2015).
- [2] Biniiaz Delijani E., Pishvaie M.R., Bozorgmehry Boozarjomehry R., [Distance Dependent Localization Approach in Oil Reservoir History Matching: A Comparative Study](#), *Iranian Journal of Chemistry and Chemical Engineering (IJCCE)*, **33**(1): 75-91 (2014).
- [3] Sadeghnejad S., Masihi M., Pishvaie M., Shojaei A., King P.R., [Utilization of Percolation Approach to Evaluate Reservoir Connectivity and Effective Permeability: A Case Study on North Pars Gas Field](#), *Scientia Iranica. Volume*, **18**(6): 1391-1396 (2011).
- [4] Sadeghnejad S., Masihi M., Pishvaie M., Shojaei A., King P.R., [Estimating the Connected Volume of Hydrocarbon During Early Reservoir Life by Percolation Theory](#), *Energy Sources, Part A: Recovery, Utilization, and Environmental Effects*, **36**(3): 301-308 (2010).
- [5] Partovi S.M.A., Sadeghnejad S., [Fractal Parameters and Well-Logs Investigation Using Automated Well-to-Well Correlation](#), *Computers & Geosciences*, **103**: 59-69 (2017).
- [6] Rivera Vega N., ["Reservoir Characterization Using Wavelet Transforms"](#), Master Thesis, Texas A&M University (2004).
- [7] Zoraster S., Paruchuri R., Darby S., ["Curve Alignment for Well-to-Well Log Correlation"](#), *SPE Annual Technical Conference and Exhibition*. Society of Petroleum Engineers (2004).
- [8] Yuan X., Guo Y., Yu Y., Shen Y., Shao Y., [Correlation and Analysis of Well-Log Sequence with Milankovitch Cycles as Rulers: A Case Study of Coal-Bearing Strata of Late Permian in Western Guizhou](#), *International Journal of Mining Science and Technology*, **23**(4): 563-568 (2013).
- [9] Perez-Muñoz T., Velasco-Hernandez J., Hernandez-Martinez E., [Wavelet Transform Analysis for Lithological Characteristics Identification in Siliciclastic Oil Fields](#), *Journal of Applied Geophysics*, **98**: 298-308 (2013).
- [10] Lapkovsky V.V., Istomin A.V., Kontorovich V.A., Berdov V.A., [Correlation of Well Logs as a Multidimensional Optimization Problem](#), *Russian Geology and Geophysics*, **56**(3): 487-492 (2015).

- [11] Dorigo M., "Optimization, Learning and Natural Algorithms", Ph. D. Thesis, Politecnico di Milano, Italy. (1992).
- [12] Lee C.Y., An Algorithm for Path Connections and Its Applications, *Electronic Computers, IRE Transactions*, (3): 346-365 (1961).
- [13] Subhakar D., Chandrasekhar E., Reservoir Characterization Using Multifractal Detrended Fluctuation Analysis of Geophysical Well-Log Data, *Physica A: Statistical Mechanics and Its Applications*, **445**: 57-65 (2016).
- [14] Ye S.-J., Wellner R.W., Dunn P.A., "Rapid and Consistent Identification of Stratigraphic Boundaries and Stacking Patterns in Well Logs-An Automated Process Utilizing Wavelet Transforms and Beta Distributions", *SPE Middle East Oil & Gas Show and Conference*. Society of Petroleum Engineers (2017).
- [15] Kadkhodaie A., Rezaee R., Intelligent Sequence Stratigraphy Through a Wavelet-Based Decomposition of Well Log Data, *Journal of Natural Gas Science and Engineering*, **40**: 38-50. 2017.
- [16] Nie L., Shouguo W., Jianwei W., Zheng L., Lin X., Rui L., Continuous Wavelet Transform and Its Application to Resolving and Quantifying the Overlapped Voltammetric Peaks, *Analytica Chimica Acta*, **450**(1): 185-192 (2001).
- [17] Misiti M., Misiti Y., Oppenheim G., Poggi J.M., *Matlab Wavelet Toolbox User's Guide. Version 3*. (2004).
- [18] Liu X., Wang H., Gu H., Fractal Characteristic Analysis of Electrochemical Noise with Wavelet Transform, *Corrosion Science*, **48**(6): 1337-1367 (2006).
- [19] Iftekharruddin K.M., Parra C., "Multiresolution-Fractal Feature Extraction and Tumor Detection: Analytical Modeling and Implementation", *Optical Science and Technology, SPIE's 48th Annual Meeting*, International Society for Optics and Photonics (2003).
- [20] Peitgen H.-O., Jürgens H., Saupe D., *Chaos and "Fractals: New Frontiers of Science"*, Springer Science & Business Media. (2006).
- [21] Riedi R.H., Crouse M.S., Riberio V.J., Baraniuk R.G., A Multifractal Wavelet Model with Application to Network, Traffic, *Information Theory, IEEE Transactions on*, **45**(3): 992-1018 (1999).
- [22] Mandelbrot B.B., Van Ness J.W., Fractional Brownian Motions, Fractional Noises and Applications. *SIAM Review*, **10**(4): 422-437 (1968).
- [23] Cavanaugh J.E., Wang Y., Davis J.W., Locally Self-Similar Processes and Their Wavelet Analysis, *Handbook of Statistics*, **21**: 93-135 (2003).
- [24] Jacquet G., Harba R., "Wavelet Based Estimator for Fractional Brownian Motion: An Experimental Point of View", *Signal Processing Conference, 2004 12th European*. IEEE (2004).
- [25] Goncalves P., Riedi R., "Wavelet Analysis of Fractional Brownian Motion in Multifractal Time. in 17^o Colloque Sur le Traitement du Signal et Des Images", *FRA, 1999*. GRETSI, Groupe d'Etudes du Traitement du Signal et des Images (1999).
- [26] Taqqu M.S., Teverovsky V., Willinger W., Estimators for Long-Range Dependence: An Empirical Study, *Fractals*, **3**(04): 785-798 (1995).
- [27] Higuchi T., Approach to an Irregular Time Series on the Basis of the Fractal Theory, *Physica D: Nonlinear Phenomena*, **31**(2): 277-283 (1988).
- [28] Beran J., "Statistics for Long-Memory Processes, volume 61 of Monographs on Statistics and Applied Probability", New York: Chapman and Hall. (1994).
- [29] Soltani S., Simard P., Boichu D., Estimation of the Self-Similarity Parameter Using the Wavelet Transform, *Signal Processing*, **84**(1): 117-123 (2004).
- [30] Turcotte D.L., "Fractals and Chaos in Geology and Geophysics", Cambridge University Press. (1997).
- [31] Sadeghnejad S., Partovi S.M.A., "Reservoir Rock Characterization Using Wavelet Transform and Fractals Analysis", *The 9th International Chemical Engineering Congress & Exhibition (ICChEC 2015)*, Shiraz, Iran (2015).
- [32] Fitch P.J.R., Lovell M.R., Davies S.J., Pritchard T., Harvey P.K., An Integrated and Quantitative Approach to Petrophysical Heterogeneity, *Marine and Petroleum Geology*, **63**: 82-96 (2015).